TRANSPLANTATION

Cord blood T cells mediate enhanced antitumor effects compared with adult peripheral blood T cells

Prashant Hiwarkar,[1,2] Waseem Qasim,[1,3] Ida Ricciardelli,[1] Kimberly Gilmour,[4] Sergio Quezada,[5] Aurore Saudemont,[6,7] Persis Amrolia,[1,8,*] and Paul Veys[1,8,*]

[1]Molecular and Cellular Immunology Section, University College London Institute of Child Health, London, United Kingdom; [2]Department of Haematology and Bone Marrow transplantation, Birmingham Children's Hospital, Birmingham, United Kingdom; [3]Department of Immunology and [4]Laboratory Immunology, Great Ormond Street Hospital for Children, London, United Kingdom; [5]Department of Haematology, University College London Cancer Institute, London, United Kingdom; [6]Anthony Nolan Research Institute, London, United Kingdom; [7]Cancer Institute, University College London, London, United Kingdom; and [8]Department of Bone Marrow Transplantation, Great Ormond Street Hospital for Children, London, United Kingdom

Key Points

- CB T cells mediate enhanced antitumor responses compared with PB T cells in a murine model of B-cell lymphoma.
- The antitumor activity correlates with increased tumor-homing of CCR7^{high} CB CD8^{+} T cells and rapid gain of cytotoxic and Th1 function.

Unrelated cord blood transplantation (CBT) without in vivo T-cell depletion is increasingly used to treat high-risk hematologic malignancies. Following T-replete CBT, naïve CB T cells undergo rapid peripheral expansion with memory-effector differentiation. Emerging data suggest that unrelated CBT, particularly in the context of HLA mismatch and a T-replete graft, may reduce leukemic relapse. To study the role of CB T cells in mediating graft-versus-tumor responses and dissect the underlying immune mechanisms for this, we compared the ability of HLA-mismatched CB and adult peripheral blood (PB) T cells to eliminate Epstein-Barr virus (EBV)-driven human B-cell lymphoma in a xenogeneic NOD/SCID/IL2rg^{null} mouse model. CB T cells mediated enhanced tumor rejection compared with equal numbers of PB T cells, leading to improved survival in the CB group ($P < .0003$). Comparison of CB T cells that were autologous vs allogeneic to the lymphoma demonstrated that this antitumor effect was mediated by alloreactive rather than EBV-specific T cells. Analysis of tumor-infiltrating lymphocytes demonstrated that CB T cells mediated this enhanced antitumor effect by rapid infiltration of the tumor with CCR7^{+}CD8^{+} T cells and prompt induction of cytotoxic CD8^{+} and CD4^{+} T-helper (Th1) T cells in the tumor microenvironment. In contrast, in the PB group, this antilymphoma effect is impaired because of delayed tumoral infiltration of PB T cells and a relative bias toward suppressive Th2 and T-regulatory cells. Our data suggest that, despite being naturally programmed toward tolerance, reconstituting T cells after unrelated T-replete CBT may provide superior Tc1-Th1 antitumor effects against high-risk hematologic malignancies. (*Blood*. 2015;126(26):2882-2891)

Introduction

Unrelated cord blood transplantation (CBT) appears to be more permissive of an HLA mismatch between the recipient and donor, with a lower risk of graft-versus-host disease (GVHD) for a given degree of mismatch compared with hematopoietic cell transplantation from adult donors.[1,2] This is likely to reflect the fact that, compared with naïve adult T cells, CB T cells are T-helper (Th)2-Tc2 biased with reduced inducible expression of Th1-Tc1 cytokines, such as interferon γ (IFN-γ).[3,4] In addition, the fetal immune system is believed to induce immune tolerance after exposure to foreign antigens.[5,6] In vivo T-cell depletion leads to delayed T-cell reconstitution after CBT, resulting in a high morbidity and mortality from infection.[7-10] We showed that omission of serotherapy leads to enhanced thymus-independent T-cell expansion of donor CB T cells.[11] This enhanced T-cell reconstitution after CBT is CD4^{+} T-cell biased, a pattern not observed after transplantation using a bone marrow or peripheral blood (PB) stem cell graft, and, intriguingly, occurs despite 1 log lower T cells in the CB graft compared with the bone marrow graft. Furthermore, these rapidly expanding naïve CB T cells differentiate into viral-specific T lymphocytes within 2 months, leading to rapid clearance of viral infections such as cytomegalovirus and adenovirus.[11] These observations suggest that, despite an intrinsic bias toward anti-inflammatory Th2-Tc2 immune responses, naive CB T cells can rapidly proliferate and differentiate into antigen-specific T lymphocytes.

In view of clinical data suggesting that CBT appears associated with a significantly lower risk of leukemic relapse, particularly after HLA-mismatched[12] and T-cell replete CBT,[13-16] we questioned whether the rapidly expanding T-cell compartment after CBT also accounts for enhanced graft-versus-leukemia (GVL) effects. To determine whether CB T cells can mediate potent antitumor effects in vivo and to elucidate the mechanism for this, we compared the ability of HLA-mismatched CB T cells vs adult PB T cells to reject Epstein-Barr virus (EBV)-driven B-cell lymphoma in a xenograft tumor model in the immunodeficient mouse strain NOD/SCID/IL2rγ^{null} (NSG). We demonstrate that CB

Submitted June 29, 2015; accepted September 28, 2015. Prepublished online as *Blood* First Edition paper, October 8, 2015; DOI 10.1182/blood-2015-06-654780.

*P.A. and P.V. contributed equally to this work.

The online version of this article contains a data supplement.

There is an Inside *Blood* Commentary on this article in this issue.

The publication costs of this article were defrayed in part by page charge payment. Therefore, and solely to indicate this fact, this article is hereby marked "advertisement" in accordance with 18 USC section 1734.

T cells mediate curative and enhanced antitumor responses compared with PB T cells.

Methods

Generation of EBV-driven B-cell lymphoma cell lines

A total of 5×10^6 freshly isolated mononuclear cells from healthy CB or PB donors were cultured with an EBV supernatant produced from the B95-8 cell line in the presence of 1 μg/mL cyclosporin A to inhibit EBV-specific T-cell responses as previously described.[17] B-cell lymphoma cell lines (LCLs) were transduced with an SFG retroviral vector encoding green shifted firefly luciferase (F-Luc) and cultured in RPMI medium with 10% fetal calf serum + 1% penicillin/streptomycin (RF10). Expression of F-Luc allows for noninvasive monitoring of xenografted tumors in mice by luminescent imaging in vivo.

T-cell selection

Mononuclear cells were separated from CB and PB using Ficoll-Paque PLUS. Negatively selected $CD3^+$ T cells were isolated using Milteyni Pan T-cell Isolation Kit, human (130-096-535) and counted using a Sysmex XE-5000 automated hematology system. The purity of negatively selected T cells was >94% (supplemental Table 2 available on the *Blood* Web site).

Xenograft model and tumor imaging

NSG mice were obtained from the Jackson Laboratory and raised under pathogen-free conditions. All animal studies were approved by the University College London Biological Services Ethical Review Committee and licensed under the Animals (Scientific Procedures) Act 1986 (Home Office, London, UK). In primary murine modeling experiments performed to study the differential GVL effect between CB and PB T cells, mice were inoculated with 5×10^6 F-Luc expressing EBV LCLs subcutaneously on the nape of the neck on day –2. To evaluate the antitumor activity, 5×10^6 comparably HLA-mismatched CB or PB $CD3^+$ T cells were injected intravenously (by tail vein injection) after 2 days on day +0 (supplemental Figure 1). HLA typing was performed for A, B, C, DRB1, and DQB1 antigens. In the first experiment, 10 of 10, and in the second experiment, 7 of 10, HLA antigens were mismatched between CB T cells vs LCLs and PB T cells vs LCLs (supplemental Table 1). Tumor growth was evaluated using the in vivo imaging system (Xenogen; Caliper Life Sciences, Hopkinton, MA). Animals were imaged on day +10, +20, +25, +30, and +35. Photon emission from $FLuc^+$ LCLs expressed in photon per second per cm^2 per steradian ($p/s/cm^2/sr$) was quantified using Living Image software (Xenogen) as previously described.[18] In addition to monitoring the tumor bioluminescence, 2-dimensional caliper measurements of the tumor were performed, and tumor volume was derived using the following formula: tumor volume = 1/2 × (length × width2). Mice were euthanized if the tumor growth exceeded the permitted threshold of 10 mm.

Secondary murine modeling experiments to study the mechanisms of the GVL effect between CB and PB T cells are shown in a schematic diagram in supplemental Figure 1.

Tumor-infiltrating lymphocytes

Tumors were minced and incubated in RF10 medium with 0.1 mg/mL collagenase A (Roche) and 60 U/mL DNase I (Sigma-Aldrich) for 30 minutes at 37°C. Tumors were then homogenized and filtered through a nylon filter (70 μm), and the lymphocytes were isolated in RF-10. Tumor-infiltrating lymphocytes (TILs) were studied for (1) IFN-γ, tumor necrosis factor (TNF)-α, and interleukin (IL)-4 responses; (2) perforin expression; and (3) naïve memory effector differentiation and FoxP3 staining,[19] as detailed in the supplemental Methods.

Histology

Immunohistochemical mouse anti-human CD3 staining of tumor sections was performed to study the extent of T-cell infiltration. Using Image J, 10 RGB images of 40× magnification for each tumor slide were converted to black and white mask output using a calibrated threshold for each stack of images, and average density of T cells per square millimeter of tumor was calculated as shown in supplemental Figure 2.[20]

Statistics

Statistical analysis was done using GraphPad Prism software. Tumor volumes of either photons/s/cm^2/sr or mm^3 are expressed as mean and standard error of mean. A two-tailed Student *t* test was performed for comparisons of experimental groups. A log-rank (Mantel-Cox) test was used to compare survival between different groups of mice.

Results

CB T cells mediate enhanced antitumor effects compared with PB T cells

We initially compared the antitumor effects of equivalent doses of T cells derived from comparably HLA-mismatched CB vs PB in a NSG mouse model of EBV-driven B-cell lymphoma. In 2 consecutive experiments where mice were treated with 5×10^6 allogeneic T cells derived from different donors 2 days after inoculation with 5×10^6 tumor cells, we observed that control mice receiving B-cell lymphoma without T cells (n = 6) and mice receiving B-cell lymphoma followed by PB T cells (n = 10) exhibited tumor growth exceeding the threshold limit of 10 mm between 20 and 22 days following tumor inoculation, so that these mice had to be euthanized. In contrast, 9 of 10 mice receiving the same dose of CB T cells showed slower tumor growth followed by complete tumor regression (Figure 1A). These findings were confirmed by measuring tumor bioluminescence in photons/s/cm^2/sr using a Xenogen-IVIS imaging system. The mean tumor bioluminescence of the CB group on day +20 was significantly lower than that of the PB and control group ($9.65 \pm 2.65 \times 10^9$ vs $3.83 \pm 1.08 \times 10^{10}$ and $3.04 \pm 0.84 \times 10^{10}$, respectively; $P < .01$; Figure 1B). These IVIS findings were mirrored by caliper-measured tumor volumes. On day +20, the mean tumor volume in the CB group was 204 mm^3 (Figure 1C), which was significantly lower than the mean tumor volume of the PB (814 mm^3) and control (812 mm^3) group ($P < .01$).

Surviving mice in the CB group were monitored for 60 days after T-cell injection without recurrence of tumor or xenogeneic GVHD. This resulted in significantly improved survival in the CB group compared with the PB group ($P < .0003$; Figure 1D). In addition to these primary in vivo imaging experiments, the superior antitumor effect of CB T cells was also observed in 2 additional functional experiments with different CB and PB T-cell donors, where tumor volumes were measured using a caliper (supplemental Figure 3). This observation suggests that CB T cells can mediate potent and enhanced graft-versus-tumor effects compared with PB T cells in this model.

CB T cells are not xenoreactive, whereas PB T-cell antitumor effects correlate with xenoreactivity

It is well established that human PB T cells can mediate xenoreactivity.[21-23] We next compared the xenoreactive capacity of 5×10^6 CB vs PB T cells in tumor-free NSG mice. In mice receiving PB T cells, we observed the onset of xenoreactivity 3 weeks following T-cell injection: all mice developed ruffled fur, lethargy, and weight loss 3 weeks after T-cell injections (supplemental Figure 4A). In contrast, mice receiving CB T cells did not develop any symptoms of xenoreactivity, despite the presence of circulating human T cells up to 60 days after injection. Xenogeneic GVHD in the PB T-cell group

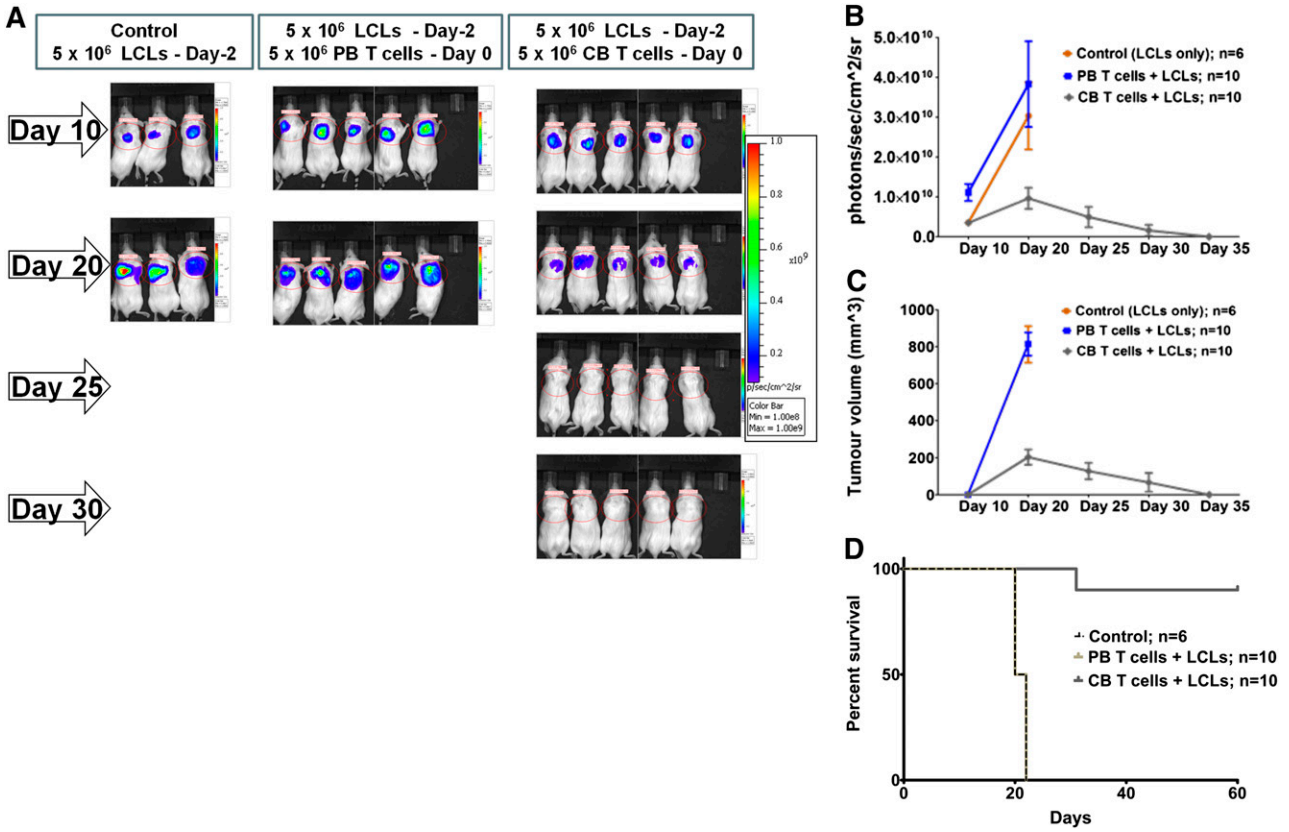

Figure 1. Cord blood T cells mediate enhanced antitumor effects compared with peripheral blood T cells. (A) Representative experiment illustrates slower tumor growth followed by rapid rejection of B-cell lymphoma in mice receiving allogeneic CB T cells compared with mice receiving allogeneic PB T cells and control mice. All images are shown on 1 scale (range, 1.00e8-1.00e9 photons/s/cm^2/sr). Tumor size in control mice and those receiving PB T cells exceeded threshold of 10 mm, and hence these mice were euthanized. (B) Tumor bioluminescence (photons/s/cm^2/sr) was measured using Xenogen-IVIS, and (C) tumor volume (mm^3) was derived using caliper measurements. Cumulative rate of tumor growth (mean and standard error of mean) from 2 separate experiments are plotted. These plots show a significantly slower rate of tumor growth in the mice receiving CB T cells compared with the mice receiving PB T cells and the control group. (D) Regression of the tumor following infusion of CB T cells led to significantly improved survival in this group compared with the PB group ($P < .0003$).

was confirmed histologically in the liver and skin with T-cell infiltration, distortion of normal architecture, and apoptotic changes around the bile ducts and in the intradermal region, but this was not seen in CB T-cell recipients (supplemental Figure 4B).

To model the antitumor effects of PB T cells and how this correlates with xenoreactivity, we performed a similar tumor modeling experiment with a lower burden of B-cell lymphoma. We injected 2.5×10^6 LCLs subcutaneously on day –2, followed by the tail vein injection of 5×10^6 PB T cells in the treatment but not the control group. We observed that the control mice had tumor growth >10 mm on day +27 after tumor inoculation, requiring these mice to be euthanized. In mice receiving PB T cells, tumors grew for the first 3 weeks with no significant difference in mean tumor bioluminescence between the tumors in the control and PB T-cell groups ($3.89 \pm 2.15 \times 10^8$ vs $5.69 \pm 1.69 \times 10^8$; P = not significant) but subsequently started regressing. This tumor regression correlated with the onset of signs of xenoreactivity such as ruffled fur, lethargy, and weight loss (supplemental Figure 5A-B).

Thus, the antitumor effect of CB T cells appears independent of xenoreactivity. PB T cells can also mediate an antitumor effect in this model, but this was attenuated compared with CB T cells and correlated with xenoreactivity.

Antitumor effects of CB T cells are mediated through alloreactivity

Because the B-cell lymphoma used in this model is an EBV-driven tumor expressing viral antigens,[24,25] we next determined whether the tumor regression observed in the CB group was due to an antiviral or an alloreactive effect. To model this, we compared the ability of 5×10^6 autologous and allogeneic CB T cells to reject LCL tumors. We observed that control mice receiving LCLs without T cells (n = 3) and mice receiving LCLs followed by autologous CB T cells (n = 5) had tumor growth exceeding the threshold limit of 10 mm on day +22 after tumor inoculation and were therefore euthanized. In contrast, mice injected with LCLs and allogeneic CB T cells (n = 5) had slower tumor growth followed by complete tumor regression. On day +22, the autologous CB T-cell group had a mean tumor volume (mm^3) and mean tumor bioluminescence (photons/s/cm^2/sr) of 1223 ± 72 and $1.32 \pm 0.25 \times 10^{11}$, respectively. In contrast to these large tumors, the mean tumor volume (mm^3) and mean tumor bioluminescence (photons/s/cm^2/sr) in the allogeneic CB T-cell group were significantly lower: 12 ± 6 and $1.80 \pm 1.09 \times 10^9$, respectively ($P < .01$; Figure 2A-C). These results indicate that the tumor regression observed with CB T cells appears to be mediated through an alloreactive rather than an EBV-specific T-cell response.

Enhanced recruitment of CB T cells to the tumor may mediate a more potent antitumor effect

To study the immunologic basis of this differential antitumor effect following the injection of CB and PB T cells, we first studied the differences in the recruitment of TILs. In a separate allogeneic LCL tumor experiment, mice receiving CB (n = 5) and PB (n = 5) T cells

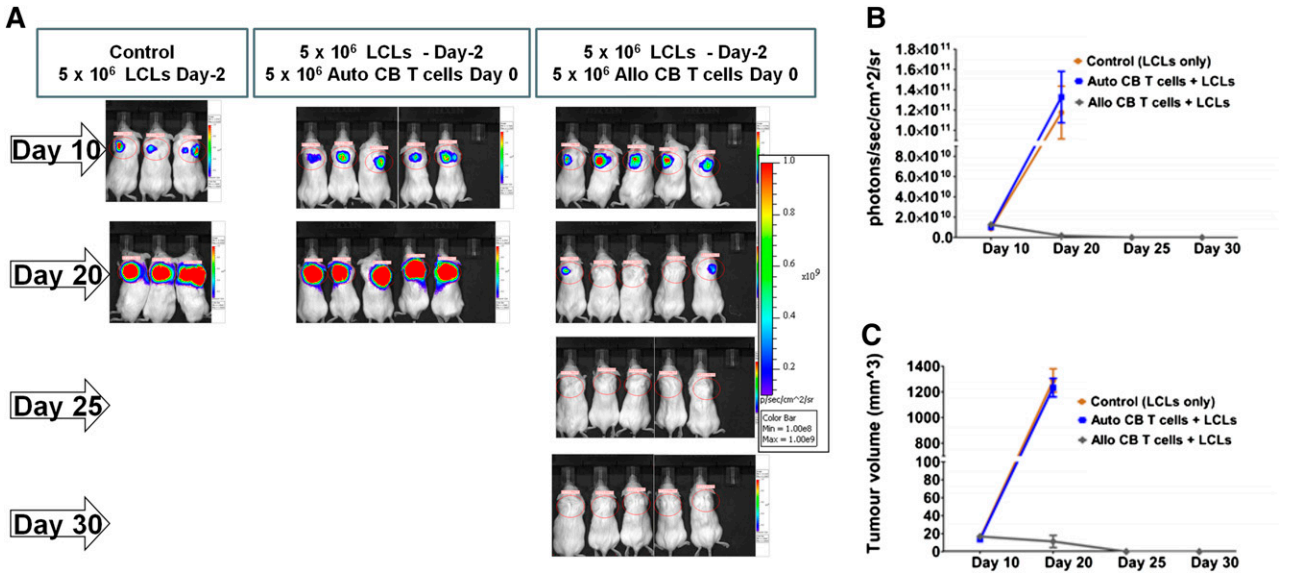

Figure 2. Antitumor effects of cord blood T cells are mediated through alloreactivity. (A) Tumor regression was observed in mice receiving allogeneic CB T cells. Tumor size in mice receiving autologous CB T cells exceeded 10 mm, and hence these mice were euthanized. This observation suggests that antitumor effects against B-cell lymphoma are an allo-reactive effect and not an EBV-specific response. All images are shown on 1 scale (range: 1.00e8-1.00e9 photons/s/cm^2/sr). (B) Tumor bioluminescence (photons/s/cm^2/sr) was measured using Xenogen-IVIS, and (C) tumor volume (mm^3) was derived using caliper measurements. Cumulative rate of tumor growth (mean and standard error of mean) are plotted.

were euthanized on day +15 following T-cell injections, and tumor sections were studied. Immunohistochemistry staining of tumor sections with CD3 antibody showed higher numbers of TILs in the CB group compared with the PB group (Figure 3A). A significantly higher number of TILs per square millimeter were observed in the CB group compared with the PB group (4702 ± 426 vs 1275 ± 330; $P <$ .01; Figure 3B). Further, flow cytometric analysis of isolated TILs showed that a majority of TILs in the CB group were CD8$^+$ T cells, with a median CD4:CD8 ratio of 0.49 (range, 0.47–0.58; Figure 3C). In contrast, CD4$^+$ T cells were predominant in the PB group, with a median CD4:CD8 ratio of 1.72 (range, 1.60-1.88; $P <$ .01). This inversion of the CD4:CD8 ratio in the CB TILs was observed despite a higher initial CD4:CD8 ratio in the injected CB T cells compared with the injected PB T cells (4.9 vs 2.9). This suggests that CB CD8$^+$ T cells are preferentially recruited to the tumor and may play a key role in mediating antitumor effects in this model.

CB TILs show a CD8$^+$ T-cell bias and higher CD8:Treg ratio than PB TILs

To further gain insight into the kinetics of infiltration of CB and PB T cells in this B-cell tumor and the role of regulatory T cells in this, we compared the infiltration of CD4$^+$, CD8$^+$, and CD4$^+$CD25$^+$FoxP3$^+$ T-regulatory cells in the tumor on day +10 and day +20 after T-cell injections. NSG mice were injected with 5 × 10^6 lymphoma cells subcutaneously followed 2 days later by 5 × 10^6 CB (n = 8) or PB T cells (n = 8). Ten and 20 days after T-cell injections, 4 mice from each group were euthanized, and isolated TILs were studied flow cytometrically for the CD4:CD8 and CD8:CD4$^+$ T-regulatory cells ratio (Figure 4A-C).

At day +10 and day +20 after T-cell injection, the median CD4:CD8 ratio in the CB TILs was 0.58 (range, 0.51-0.69) and 0.03 (range, 0.03-0.06), respectively, compared with a median ratio of 1.54 (range, 1.3-1.9) and 0.26 (range, 0.14-0.33) in the PB TILs ($P <$ .001 and $P <$ .001, respectively; Figure 4D). Thus, as previously observed, the CD4:CD8 ratio in the CB TILs was significantly reversed compared with PB TILs, despite a higher initial CD4:CD8 ratio in the injected CB T cells compared with the injected PB T cells (3.4 vs 2.7).

Similarly, at day +10 and day +20 after T-cell injection, the median CD8:CD4$^+$CD25$^+$FoxP3$^+$ ratio in the CB TILs was 29 (range, 25-52) and 2043 (range, 950-3288), respectively, compared with a median ratio of 11.9 (range, 7.8-15.5) and 132 (range, 72-166) in the PB TILs ($P <$ .01 and $P <$ .01, respectively; Figure 4D). This observation was complemented by the observed persistence of FoxP3 positivity in 3-dimensional color inspector images of 10× tumor sections in the PB group but not in the CB group (supplemental Figure 6). This differential pattern of T-cell infiltration indicate that, although CB CD8$^+$ T cells may be the primary mediators of the enhanced antitumor effect in the CB group, a relatively increased recruitment of T-regulatory cells compared with cytolytic effectors may also attenuate the antitumor effect in the PB group.

CCR7-enriched CB CD8$^+$ T cells have enhanced tumor-homing ability

Because the vast majority of CB CD8$^+$ T cells are CCR7^{high} (Figure 5A) and CCR7 is a homing receptor for naïve T cells,[26-28] we sought to identify whether CCR7$^+$CD8$^+$ T cells predominantly infiltrate the tumor.

We observed that CCR7 expression was similar in CB and PB CD8$^+$ TILs (median, fluorescence intensity [MFI] = 6854 ± 1542 vs 6737 ± 1626; P = not significant). CCR7 MFI expression was significantly higher in TILs compared with circulating PB CD8$^+$ T cells (1378 ± 10; $P < 0.01$), whereas circulating CB CD8$^+$ T cells remained CCR7^{high} (MFI = 21 128 ± 534; Figure 5B-C). This indicates that CCR7^{high} CD8$^+$ T cells were primarily recruited to the tumor, and higher expression of CCR7 may endow CB CD8$^+$ T cells with the enhanced tumor-homing ability.

Tumor-infiltrating naïve CB T cells rapidly differentiate into memory/effector cells and gain IFN-γ and TNF-α functions

For naïve CB T cells infiltrating the tumor to exert antitumor effects, they must undergo memory effector differentiation. Therefore, we studied the memory phenotype of TILs and circulating lymphocytes (CLs). We observed that TILs in the CB group rapidly underwent

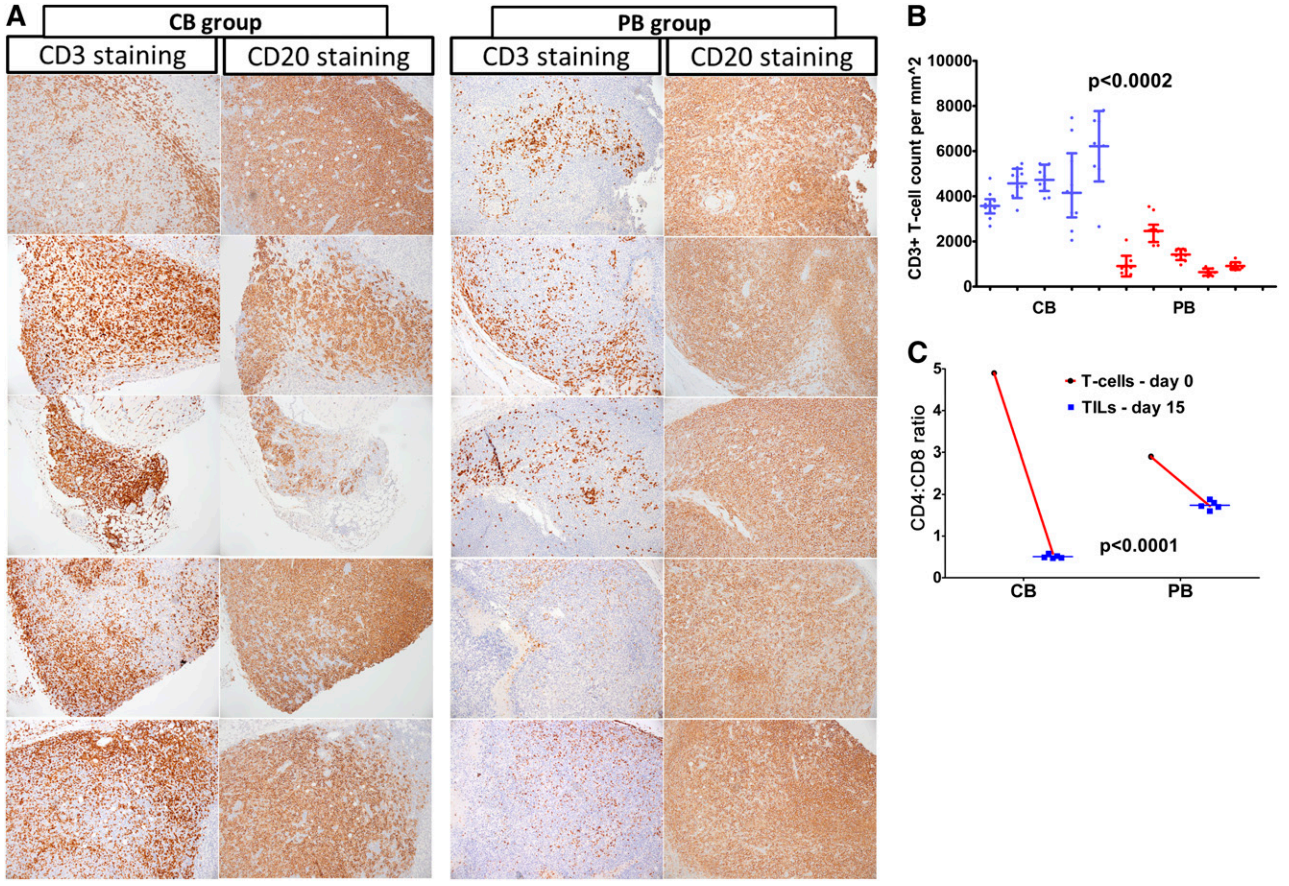

Figure 3. Cord blood T cells are rapidly recruited to the tumor compared with peripheral blood T cells. (A) Contiguous tumor sections (×10) of the CB and PB groups stained with CD3 and CD20 immuno-histochemical stain. Higher numbers of tumor-infiltrating $CD3^+$ T cells were seen in the CB group compared with the PB group. (B) Density of tumor-infiltrating T cells per square millimeter (shown as scatter dot plot with median and interquartile range) was significantly higher in the CB group than in the PB group. Importantly, as shown in C, a significantly lower CD4:CD8 ratio was observed in CB TILs compared with PB TILs, suggesting higher numbers of $CD8^+$ T cells infiltrated the tumor in the CB group compared with the PB group.

differentiation to central memory (CM) and effector memory (EM) T cells, whereas circulating CB T cells remained naïve (Figure 6A-B). A similar percentage of $CD8^+$ TILs were observed to have a CM and EM phenotype in the groups receiving CB and PB T cells (CM = 77.8 ± 1.4 vs 78.0 ± 1.8; EM = 1.48 ± 0.3 vs 2.1 ± 0.5; P = not significant).

Finally, mice in the PB (n = 5) and CB (n = 5) groups were euthanized after the onset of tumor regression in both the groups (day +26 after the injection of T cells), and isolated TILs were studied for differences in effector functions.

$CD8^+$ TILs in both the groups demonstrated IFN-γ responses, and there was no difference in the percentage of $CD8^+$ TILs expressing IFN-γ responses in the 2 groups (3.5 ± 0.14 vs 3.4 ± 0.15; P = not significant; Figure 7A). In contrast, a significantly higher percentage of CB $CD8^+$ TILs acquired TNF-α responses (1.2 ± 0.07 vs 0.48 ± 0.06; $P < .0001$; Figure 7B). Likewise, both the percentage of $CD8^+$ T cells expressing perforin and the MFI were significantly higher in CB $CD8^+$ TILs compared with PB $CD8^+$ TILs (MFI = 443 ± 16 vs 365 ± 13; percentage of $CD8^+$ T cells = 75 ± 3.0 vs 58 ± 5.0; $P < .01$; Figure 7C). Thus, CB $CD8^+$ TILs rapidly acquire higher TNF-α and perforin effector functions than PB T cells in the tumor microenvironment.

We also studied the effector functions of $CD4^+$ TILs to gain insight into the role of intratumoral Th1/Th2 balance on differential antitumor effects. A significantly higher percentage of $CD4^+$ TILs were identified as Th2 TILs in the PB group compared with the CB group (16 ± 2.0 vs 6.2 ± 1.0; $P < .001$; supplemental Figure 7A-B). Th1/Th2 balance measured as the IFN-γ/IL-4 and TNF-α/IL-4 ratios was significantly biased toward Th1 in the CB group compared with the PB group (0.98 ± 0.2 vs 0.3 ± 0.06 and 0.88 ± 0.05 vs 0.39 ± 0.07; $P < .05$ and $P < .0001$, respectively; supplemental Figure 6C-F). Thus, CB $CD4^+$ TILs gained Th1-biased responses in the tumor microenvironment.

Taken together, these observations indicate that naïve CB T cells can swiftly undergo memory effector differentiation and gain cytotoxic effector functions in the tumor microenvironment.

Discussion

Unrelated CBT is increasingly used to treat high-risk hematologic malignancies.[12,13] It is therefore critical to determine whether the rapidly expanding donor T cells following T-replete CBT can confer differential GVL effects compared with donor T cells transferred with adult stem cell sources, despite an intrinsic Tc2-Th2 bias in the CB T cells.[3,4] We therefore compared the ability of CB vs adult PB T cells to mediate an antitumor effect against the EBV-driven B-cell lymphoma in NSG mice. In this model, we observed that CB T cells mediate enhanced antitumor effects compared with PB T cells, resulting in improved survival of mice receiving CB T cells. As previously described by other groups,[29] CB T cells were not xenoreactive, and tumor regression was associated with alloreactivity rather than

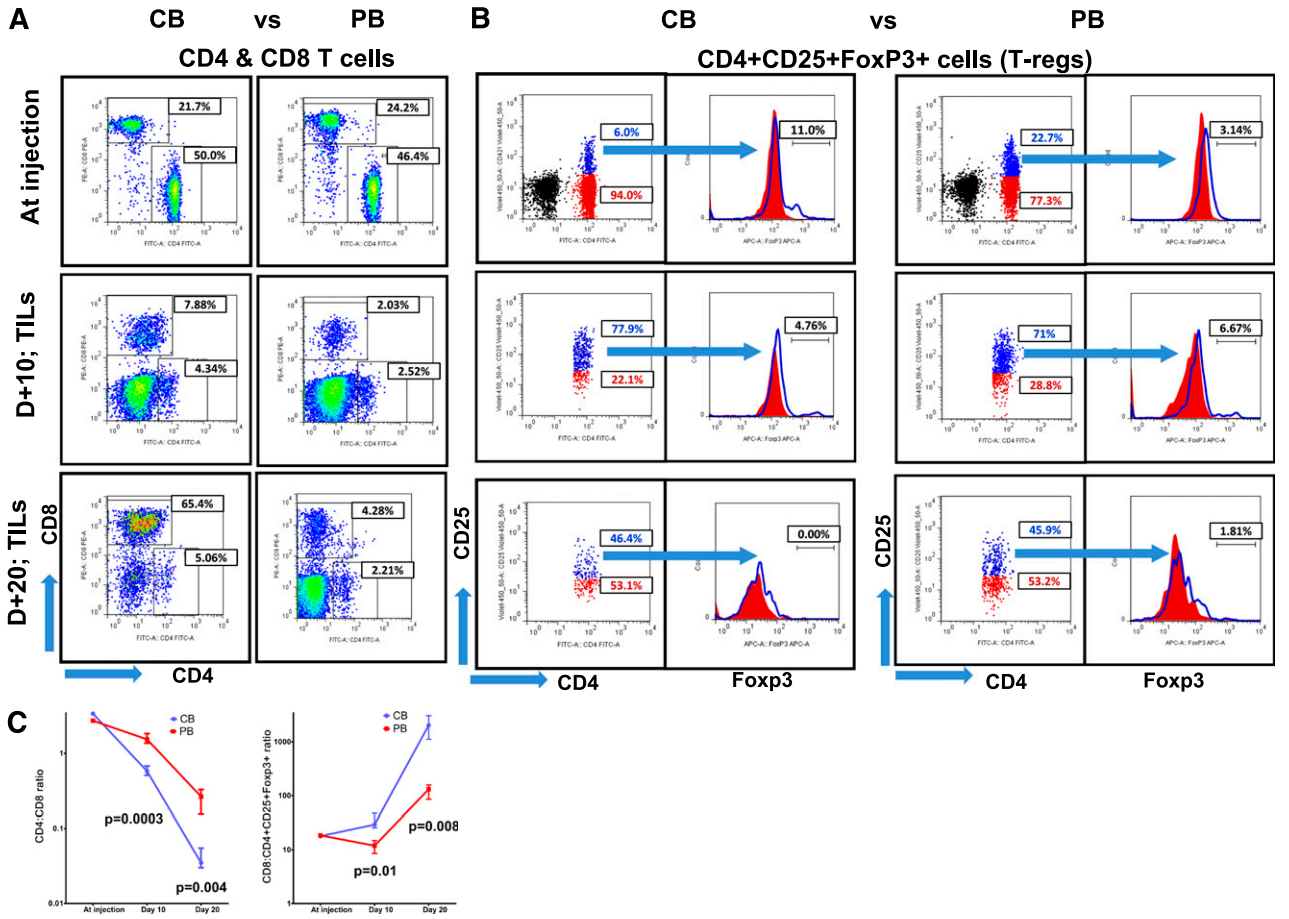

Figure 4. Cord blood TILs show a significant CD8$^+$ T-cell bias and higher CD8:T-reg ratio than peripheral blood TILs. Representative flow cytometry plots of (A) CD4$^+$ and CD8$^+$ T cells and (B) CD4$^+$CD25$^+$Foxp3$^+$ T cells at injection and in TILs on day +10 and day +20 are shown. (C) CB TILs had a significantly lower CD4:CD8 ratio and a significantly higher CD8:CD4$^+$ T-regulatory ratio compared with PB TILs on day +10 and day +20 after T-cell injection. The ratios are plotted on a log-scale as median and interquartile range.

recognition of EBV antigens. In the primary in vivo tumor imaging experiments, the superior antitumor effect observed with CB T cells is unlikely to reflect differences in HLA mismatch between the PB and CB T cells, as T cells from both sources were comparably mismatched with the LCLs, and the effect was observed with 2 different donor-recipient pairs. One limitation of our model is that both CB and PB

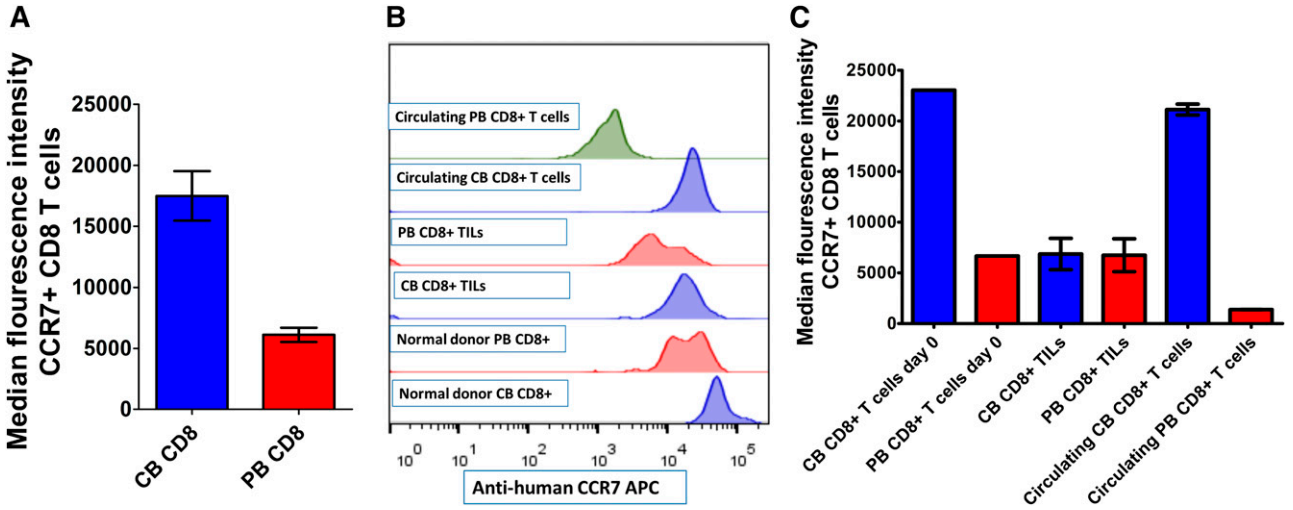

Figure 5. CCR7 enriched CB CD8$^+$ T cells have enhanced tumor-homing ability. (A) Normal donor CB CD8$^+$ T cells have significantly higher expression of CCR7 compared with normal donor PB CD8$^+$ T cells (expressed as mean and standard error of mean; n = 3 in each group; $P < .005$). (B) Offset histogram plot and (C) cumulative bar plot (mean and standard error of mean) showing fluorescence intensity of CD8$^+$ T cells from normal donors and TILs and in circulation. This figure indicates that CCR7^{high}CD8$^+$ T cells are primarily recruited to the tumor in both groups (P = not significant), and in the PB group, CCR7^{low}CD8$^+$ T cells remain in circulation ($P < .01$), indicating a role of CCR7-mediated chemotaxis in this tumor model.

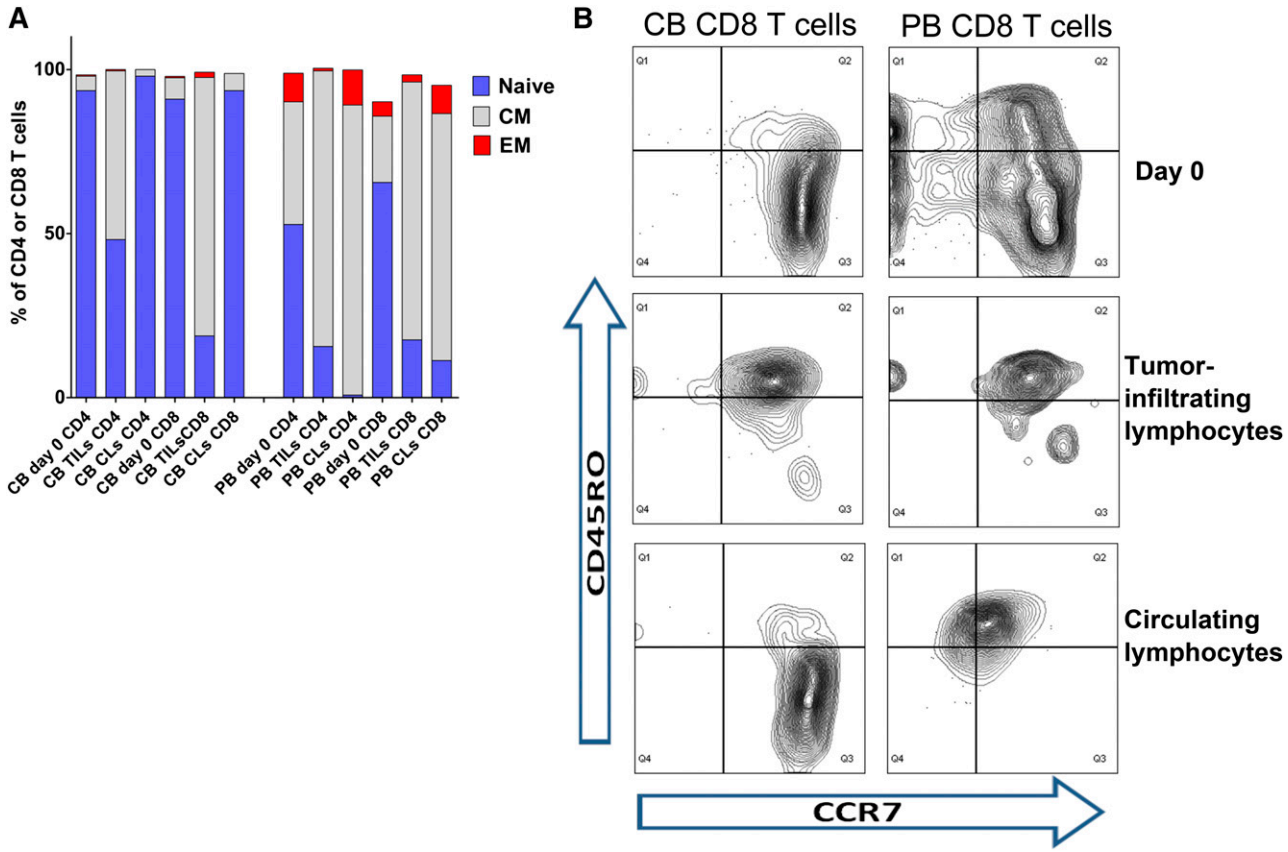

Figure 6. Tumor-infiltrating naive CB T cells rapidly differentiate into memory/effector cells. (A) Comparison of median percentages of naive, central memory, and effector memory subsets in TILs and CLs on day +15 after T-cell injection. Naive CB T cells rapidly switched to the memory/effector phenotype in the tumor; however, circulating CB lymphocytes remained naive. A similar percentage of $CD8^+$ TILs had central memory and effector memory phenotypes in both groups (P = not significant). Interestingly, in the PB group, a significantly higher percentage of CLs had an effector memory phenotype compared with TILs ($P < .0001$). (B) Representative flow cytometry plots of $CD8^+$ T cells infused on day 0, $CD8^+$ tumor-infiltrating lymphocytes, and $CD8^+$ circulating lymphocytes.

T cells were highly (7-10 of 10) mismatched with the LCL tumor, and ideally these experiments should be repeated with a more clinically relevant degree of HLA matching (ie, 0-2 mismatches) but we were unable to source CB units closely matched to the LCL tumor cells. However, we plan to perform these experiment if such CB units become available in future. The difference in antitumor effect mediated by CB and PB T cells correlated with enhanced tumoral recruitment of CB T cells compared with PB T cells. Analysis of TILs demonstrated that, after adoptive transfer of CB T cells, $CD8^+$ T cells rapidly infiltrate the tumor with induction of cytotoxic $CD8^+$ and Th1 $CD4^+$ responses in the tumor microenvironment. In contrast, in the PB group, this antitumor effect appears attenuated because of delayed tumoral infiltration of PB T cells and a relative bias toward suppressive Th2 and T-regulatory cells.

Despite the strong expression of both major histocompatibility complex class I and II in this lymphoma and the fact that both CB $CD4^+$ and $CD8^+$ T cells proliferate robustly in response to stimulation with allogeneic LCL in vitro, the majority of T cells recruited to the tumor after transfer of CB T cells were from the $CD8^+$ subset. The role of $CD8^+$ TILs in tumor immunology has been demonstrated in numerous murine models and also in cancer patients, including those with leukemia.[30-40] In a murine model of allogeneic bone marrow transplantation for acute T-cell leukemia[39] and chronic myeloid leukemia,[40] infusion of mixed donor $CD4^+$ and $CD8^+$ T cells or donor $CD8^+$ T cells alone mediated a potent GVL effect, whereas GVL was not observed with donor $CD4^+$ T cells alone. It is therefore apparent that $CD8^+$ T cells are critical as antileukemic effectors at the tumor site. Hence, in our model, the observation of the preferential infiltration of CB $CD8^+$ TILs compared with PB $CD8^+$ TILs suggests that CB $CD8^+$ T cells mediate the observed enhanced antitumor responses.

Despite the naïve phenotype of CB T cells, we observed a similar percentage of CM and EM $CD8^+$ T cells in the CB and PB TILs. Interestingly, circulating CB T cells did not undergo memory effector differentiation, in contrast to circulating PB T cells, which showed an increased percentage of EM T cells compared with PB TILs. These findings suggest that naïve CB T cells rapidly undergo memory effector differentiation within the tumor microenvironment, whereas circulating CB T cells retain a naïve phenotype.

Naïve CB $CD8^+$ T cells rapidly gained effector activity including expression of IFN-γ, TNF-α, and perforin in the tumor microenvironment. We observed similar percentages of IFN-γ–secreting $CD8^+$ TILs in the CB and PB groups, whereas the percentage of TNF-α–secreting and perforin-expressing $CD8^+$ TILs was significantly higher in the CB group. In contrast to the cytotoxic $CD8^+$ T-cell bias in the CB TILs, a preponderance of $CD4^+$ TILs was observed in the PB group with a relative bias toward suppressive Th2 and T-regulatory cells. Although $CD8^+$ TILs may primarily mediate cytotoxic antitumor effects, the Th1/Th2 balance of $CD4^+$ TILs is also important in mediating tumor-specific immune responses.[41-45] In general, immune deviation toward Th1 effectors mediates an antitumor response, whereas Th2 responses prevent tumor rejection. The relative skewing of Th1/Th2 intratumoral

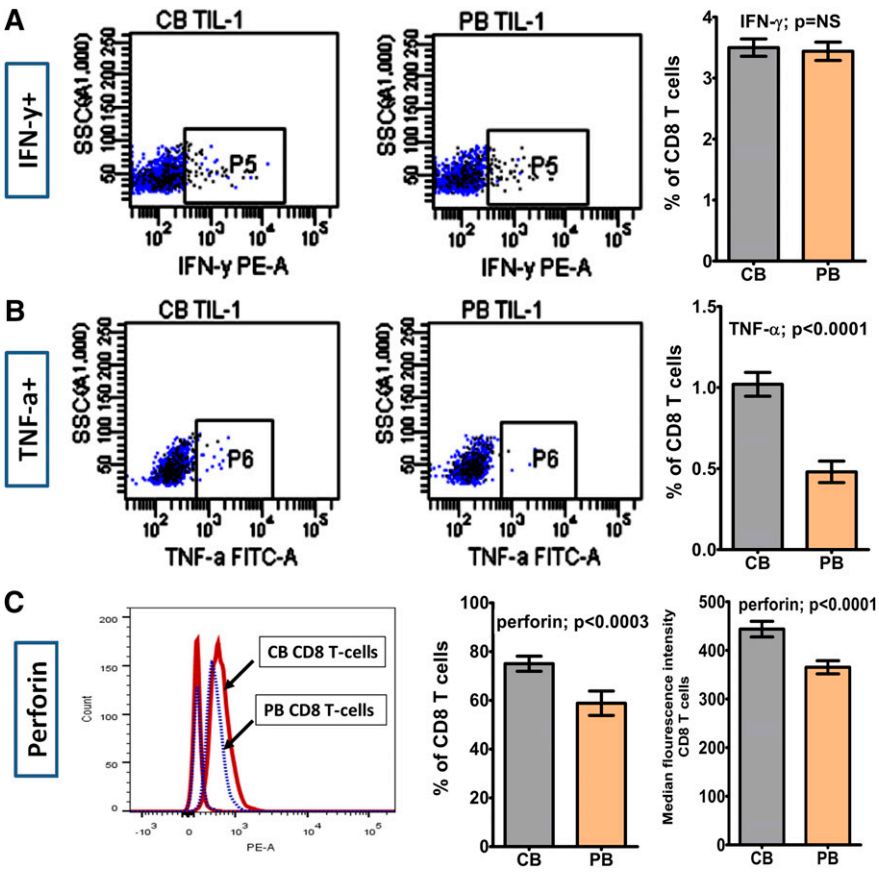

Figure 7. Tumor-infiltrating naive CB T cells rapidly gain effector functions such as IFN-γ, TNF-α and perforin. (A-C) Representative flow cytometry dot plots and cumulative bar plots (mean and standard error of mean) of percentages of CB and PB $CD8^+$ TILs secreting IFN-γ, TNF-α, and perforin expression. Although no statistically significant differences were observed in the percentage of IFN-γ–secreting $CD8^+$ TILs in the 2 groups, a significantly higher percentage of $CD8^+$ TILs in the CB group secreted TNF-α. Perforin expression was also significantly higher in the CB $CD8^+$ TILs than PB $CD8^+$ TILs and is depicted as median fluorescence intensity and percentage of $CD8^+$ TILs.

balance toward Th1 in the CB TILs is noteworthy, because this occurred despite the fact that naïve CB $CD4^+$ T cells are reported to be physiologically biased toward Th2, produce lower levels of IFN-γ than adult naïve T cells in vitro, and are hypermethylated at cytosine guanine dinucleotide and non-cytosine guanine dinucleotide sites within the IFN-γ promoter.[4] This therefore suggests that CB $CD4^+$ T cells can rapidly mature into Th1 effectors in the tumor microenvironment. Similarly, despite the immune-tolerant ontogeny of fetus,[5,6] the $CD8^+$ T cell/$CD4^+$ T-regulatory balance was significantly skewed toward $CD8^+$ T cells in the CB TILs. The immunosuppressive role of $FoxP3^+$ regulatory T cells as a crucial tumor immune-evading mechanism is well established.[46-49] In a meta-analysis of TILs in cancer sections, although $CD3^+$ and $CD8^+$ TILs were associated with good prognosis and improved survival, the $CD8^+$/$FoxP3^+$ ratio produced a more impressive hazard ratio compared with $CD3^+$ or $CD8^+$ TILs alone.[50] The enhanced GVL effect after infusion of $CD4^+$ $CD25^+$ regulatory T cell-depleted donor lymphocytes has been demonstrated further, indicating immune-evading role of T-regulatory cells following allogeneic transplantation.[51] Thus, Th1 $CD4^+$ T cells may synergize with tumor infiltrating $CD8^+$ cytotoxic effectors to enhance antitumor effects after transfer of CB T cells, whereas the relative Th2 bias and increased number of tumor-infiltrating T-regulatory cells in the PB group may impair tumor rejection in this model.

The mechanisms by which CB T cells are recruited to the tumor, proliferate preferentially in the tumor microenvironment, and mediate enhanced antitumor effects in this model remain to be elucidated, and this will require further work. CB $CD8^+$ T cells are predominantly $CCR7^{high}$ compared with a mix of $CCR7^{high}$ and $CCR7^{low}CD8^+$ T cells in the PB. The $CD8^+$ T cells homing into the tumor in both the CB and PB groups were $CCR7^{high}$, whereas $CCR7^{low}CD8^+$ T cells from the PB group remained in circulation. It is thus possible that high expression of chemokine receptor CCR7 in CB $CD8^+$ T cells may facilitate enhanced tumor homing. We therefore plan to optimize disruption of CCR7 receptor in the CB T cells using the CRISPR/Cas9 system to more closely define the role of CCR7 receptor in tumor homing.

More broadly, there is growing evidence that fetal and adult T cells are functionally distinct populations with different gene expression profiles arising from different ontogenic populations of hematopoietic stem cells.[52,53] Our as yet unpublished results indicate that the early adaptive immune system derived after T-replete CBT recapitulates a distinct molecular program of fetal ontogeny. Thus, these ontogenic differences between CB and PB T cells may not only endow CB T cells with the ability to rapidly reconstitute in the lymphopenic host following CBT,[11] but may also confer CB T cells with the ability to rapidly infiltrate the tumor and activate and differentiate in the tumor microenvironment.

In summary, CB T cells mediate more potent antitumor effects than adult T cells in this B-cell lymphoma model through enhanced recruitment of naïve CB T cells (particularly CB $CD8^+$ T cells), prompt induction of memory effector differentiation, and gain of cytotoxic effector functions in the tumor microenvironment. The findings that CB T cells mediated an enhanced GVL effect without exhibiting xenoreactivity parallel the clinical situation in humans where CBT may exert a powerful GVL effect yet with reduced rates of GVHD. Our work thus supports omission or minimization of serotherapy from the preparative regimens of CBT recipients for high-risk hematologic malignancies to enhance T cell-mediated GVL. Although we recognize the limitations in extrapolating from this model

system to the clinical setting and that other immune cells such as natural killer cells following CB grafts may also mediate a GVL effect,[54,55] these findings nonetheless provide a mechanistic insight into how CB T cells may mediate the potent GVL effects observed after T-replete CBT.

Acknowledgments

The authors thank Nick Davies, Mike Blundell, and the staff at University College London Biological Services for assistance with animal handling and Dale Moulding for assistance with Image J analysis.

This work was supported by Bloodwise (Leukaemia and Lymphoma Research), the Olivia Hodson Cancer fund, Great Ormond Street Hospital Children's Charity, and National Institute for Health Research Biomedical Research Centre at Great Ormond Street Hospital.

Authorship

Contribution: P.H., W.Q., I.R., K.G., S.Q., A.S., P.A., and P.V. designed research; P.H. and I.R. performed experiments; P.H. analyzed the data and performed statistical analysis; and P.H., W.Q., P.A., and P.V. wrote the manuscript.

Conflict-of-interest disclosure: The authors declare no competing financial interests.

Correspondence: Prashant Hiwarkar, Department of Haematology and Bone Marrow transplantation, Birmingham Children's Hospital, Steelhouse Lane, Birmingham B4 6NH, United Kingdom; e-mail: prashant.hiwarkar@bch.nhs.uk.

References

1. Rubinstein P, Carrier C, Scaradavou A, et al. Outcomes among 562 recipients of placental-blood transplants from unrelated donors. *N Engl J Med.* 1998;339(22):1565-1577.
2. Rocha V, Cornish J, Sievers EL, et al. Comparison of outcomes of unrelated bone marrow and umbilical cord blood transplants in children with acute leukemia. *Blood.* 2001;97(10): 2962-2971.
3. Marchant A, Goldman M. T cell-mediated immune responses in human newborns: ready to learn? *Clin Exp Immunol.* 2005;141(1):10-18[Review].
4. White GP, Watt PM, Holt BJ, Holt PG. Differential patterns of methylation of the IFN-gamma promoter at CpG and non-CpG sites underlie differences in IFN-gamma gene expression between human neonatal and adult CD45RO- T cells. *J Immunol.* 2002;168(6):2820-2827.
5. Silverstein AM. Ontogeny of the immune response. *Science.* 1964;144(3625):1423-1428.
6. Silverstein AM, Prendergast RA, Kraner KL. Fetal response to antigenic stimulus. IV. Rejection of skin homografts by the fetal lamb. *J Exp Med.* 1964;119:955-964.
7. Gluckman E, Rocha V, Boyer-Chammard A, et al; Eurocord Transplant Group and the European Blood and Marrow Transplantation Group. Outcome of cord-blood transplantation from related and unrelated donors. *N Engl J Med.* 1997;337(6):373-381.
8. Brunstein CG, Weisdorf DJ, DeFor T, et al. Marked increased risk of Epstein-Barr virus-related complications with the addition of antithymocyte globulin to a nonmyeloablative conditioning prior to unrelated umbilical cord blood transplantation. *Blood.* 2006;108(8):2874-2880.
9. Lindemans CA, Chiesa R, Amrolia PJ, et al. Impact of thymoglobulin prior to pediatric unrelated umbilical cord blood transplantation on immune reconstitution and clinical outcome. *Blood.* 2014;123(1):126-132.
10. Admiraal R, van Kesteren C, Jol-van der Zijde CM, et al. Association between anti-thymocyte globulin exposure and CD4+ immune reconstitution in paediatric haemopoietic cell transplantation: a multicentre, retrospective pharmacodynamic cohort analysis. *Lancet Haematol.* 2015;2(5):e194-e203.
11. Chiesa R, Gilmour K, Qasim W, et al. Omission of in vivo T-cell depletion promotes rapid expansion of naïve CD4+ cord blood lymphocytes and restores adaptive immunity within 2 months after unrelated cord blood transplant. *Br J Haematol.* 2012;156(5):656-666.
12. Eapen M, Rubinstein P, Zhang MJ, et al. Outcomes of transplantation of unrelated donor umbilical cord blood and bone marrow in children with acute leukaemia: a comparison study. *Lancet.* 2007;369(9577):1947-1954.
13. Zheng C, Luan Z, Fang J, et al. Comparison of conditioning regimens with or without antithymocyte globulin for unrelated cord blood transplantation in children with high-risk or advanced hematological malignancies. *Biol Blood Marrow Transplant.* 2015;21(4):707-712.
14. Wagner JE Jr, Eapen M, Carter S, et al; Blood and Marrow Transplant Clinical Trials Network. One-unit versus two-unit cord-blood transplantation for hematologic cancers. *N Engl J Med.* 2014;371(18):1685-1694.
15. Brunstein CG, Fuchs EJ, Carter SL, et al; Blood and Marrow Transplant Clinical Trials Network. Alternative donor transplantation after reduced intensity conditioning: results of parallel phase 2 trials using partially HLA-mismatched related bone marrow or unrelated double umbilical cord blood grafts. *Blood.* 2011;118(2):282-288.
16. Barker JN, Fei M, Karanes C, et al; RCI BMT 05-DCB Protocol Team. Results of a prospective multicentre myeloablative double-unit cord blood transplantation trial in adult patients with acute leukaemia and myelodysplasia. *Br J Haematol.* 2015;168(3):405-412.
17. Comoli P, Labirio M, Basso S, et al. Infusion of autologous Epstein-Barr virus (EBV)-specific cytotoxic T cells for prevention of EBV-related lymphoproliferative disorder in solid organ transplant recipients with evidence of active virus replication. *Blood.* 2002;99(7):2592-2598.
18. Savoldo B, Rooney CM, Di Stasi A, et al. Epstein Barr virus specific cytotoxic T lymphocytes expressing the anti-CD30zeta artificial chimeric T-cell receptor for immunotherapy of Hodgkin disease. *Blood.* 2007;110(7):2620-2630.
19. Law JP, Hirschkorn DF, Owen RE, Biswas HH, Norris PJ, Lanteri MC. The importance of Foxp3 antibody and fixation/permeabilization buffer combinations in identifying CD4+CD25+Foxp3+ regulatory T cells. *Cytometry A.* 2009;75(12): 1040-1050.
20. Loughlin PM, Cooke TG, George WD, Gray AJ, Stott DI, Going JJ. Quantifying tumour-infiltrating lymphocyte subsets: a practical immuno-histochemical method. *J Immunol Methods.* 2007;321(1-2):32-40.
21. King MA, Covassin L, Brehm MA, et al. Human peripheral blood leucocyte non-obese diabetic-severe combined immunodeficiency interleukin-2 receptor gamma chain gene mouse model of xenogeneic graft-versus-host-like disease and the role of host major histocompatibility complex. *Clin Exp Immunol.* 2009;157(1):104-118.
22. Ali N, Flutter B, Sanchez Rodriguez R, et al. Xenogeneic graft-versus-host-disease in NOD-scid IL-2Rγnull mice display a T-effector memory phenotype. *PLoS One.* 2012;7(8):e44219.
23. Covassin L, Laning J, Abdi R, et al. Human peripheral blood CD4 T cell-engrafted non-obese diabetic-scid IL2rγ(null) H2-Ab1 (tm1Gru) Tg (human leucocyte antigen D-related 4) mice: a mouse model of human allogeneic graft-versus-host disease. *Clin Exp Immunol.* 2011;166(2): 269-280.
24. Maruo S, Wu Y, Ishikawa S, Kanda T, Iwakiri D, Takada K. Epstein-Barr virus nuclear protein EBNA3C is required for cell cycle progression and growth maintenance of lymphoblastoid cells. *Proc Natl Acad Sci USA.* 2006;103(51):19500-19505.
25. Maruo S, Johannsen E, Illanes D, Cooper A, Kieff E. Epstein-Barr Virus nuclear protein EBNA3A is critical for maintaining lymphoblastoid cell line growth. *J Virol.* 2003;77(19):10437-10447.
26. De Waele M, Foulon W, Renmans W, et al. Hematologic values and lymphocyte subsets in fetal blood. *Am J Clin Pathol.* 1988;89(6):742-746.
27. Zhao Y, Dai ZP, Lv P, Gao XM. Phenotypic and functional analysis of human T lymphocytes in early second- and third-trimester fetuses. *Clin Exp Immunol.* 2002;129(2):302-308.
28. Förster R, Schubel A, Breitfeld D, et al. CCR7 coordinates the primary immune response by establishing functional microenvironments in secondary lymphoid organs. *Cell.* 1999;99(1): 23-33.
29. Leung W, Ramírez M, Mukherjee G, et al. Comparisons of alloreactive potential of clinical hematopoietic grafts. *Transplantation.* 1999; 68(5):628-635.
30. Zhang L, Conejo-Garcia JR, Katsaros D, et al. Intratumoral T cells, recurrence, and survival in epithelial ovarian cancer. *N Engl J Med.* 2003; 348(3):203-213.
31. Sato E, Olson SH, Ahn J, et al. Intraepithelial CD8+ tumor-infiltrating lymphocytes and a high CD8+/regulatory T cell ratio are associated with favorable prognosis in ovarian cancer. *Proc Natl Acad Sci USA.* 2005;102(51):18538-18543.
32. Galon J, Costes A, Sanchez-Cabo F, et al. Type, density, and location of immune cells within human colorectal tumors predict clinical outcome. *Science.* 2006;313(5795):1960-1964.
33. Leffers N, Gooden MJ, de Jong RA, et al. Prognostic significance of tumor-infiltrating

T-lymphocytes in primary and metastatic lesions of advanced stage ovarian cancer. *Cancer Immunol Immunother.* 2009;58(3):449-459.

34. Fearon ER, Pardoll DM, Itaya T, et al. Interleukin-2 production by tumor cells bypasses T helper function in the generation of an antitumor response. *Cell.* 1990;60(3):397-403.
35. Dranoff G, Jaffee E, Lazenby A, et al. Vaccination with irradiated tumor cells engineered to secrete murine granulocyte-macrophage colony-stimulating factor stimulates potent, specific, and long-lasting anti-tumor immunity. *Proc Natl Acad Sci USA.* 1993;90(8):3539-3543.
36. Han S, Zhang C, Li Q, et al. Tumour-infiltrating CD4(+) and CD8(+) lymphocytes as predictors of clinical outcome in glioma. *Br J Cancer.* 2014; 110(10):2560-2568.
37. Liang Y, Huang T, Zhang C, et al. Donor CD8+ T cells facilitate induction of chimerism and tolerance without GVHD in autoimmune NOD mice conditioned with anti-CD3 mAb. *Blood.* 2005;105(5):2180-2188.
38. Zhang C, Lou J, Li N, et al. Donor CD8+ T cells mediate graft-versus-leukemia activity without clinical signs of graft-versus-host disease in recipients conditioned with anti-CD3 monoclonal antibody. *J Immunol.* 2007;178(2):838-850.
39. Johnson BD, Becker EE, Truitt RL. Graft-vs.-host and graft-vs.-leukemia reactions after delayed infusions of donor T-subsets. *Biol Blood Marrow Transplant.* 1999;5(3):123-132.
40. Lu YF, Gavrilescu LC, Betancur M, Lazarides K, Klingemann H, Van Etten RA. Distinct graft-versus-leukemic stem cell effects of early or delayed donor leukocyte infusions in a mouse chronic myeloid leukemia model. *Blood.* 2012; 119(1):273-284.
41. Tsung K, Meko JB, Peplinski GR, Tsung YL, Norton JA. IL-12 induces T helper 1-directed antitumor response. *J Immunol.* 1997;158(7): 3359-3365.
42. Aruga A, Aruga E, Tanigawa K, Bishop DK, Sondak VK, Chang AE. Type 1 versus type 2 cytokine release by Vbeta T cell subpopulations determines in vivo antitumor reactivity: IL-10 mediates a suppressive role. *J Immunol.* 1997; 159(2):664-673.
43. Fowler DH, Breglio J, Nagel G, Hirose C, Gress RE. Allospecific CD4+, Th1/Th2 and CD8+, Tc1/Tc2 populations in murine GVL: type I cells generate GVL and type II cells abrogate GVL. *Biol Blood Marrow Transplant.* 1996;2(3):118-125.
44. Blazar BR, Taylor PA, Panoskaltsis-Mortari A, Vallera DA. Rapamycin inhibits the generation of graft-versus-host disease- and graft-versus-leukemia-causing T cells by interfering with the production of Th1 or Th1 cytotoxic cytokines. *J Immunol.* 1998;160(11):5355-5365.
45. Hu HM, Urba WJ, Fox BA. Gene-modified tumor vaccine with therapeutic potential shifts tumor-specific T cell response from a type 2 to a type 1 cytokine profile. *J Immunol.* 1998;161(6): 3033-3041.
46. Dunn GP, Old LJ, Schreiber RD. The immunobiology of cancer immunosurveillance and immunoediting. *Immunity.* 2004;21(2):137-148.
47. Shevach EM. CD4+ CD25+ suppressor T cells: more questions than answers. *Nat Rev Immunol.* 2002;2(6):389-400.
48. Zou W. Immunosuppressive networks in the tumour environment and their therapeutic relevance. *Nat Rev Cancer.* 2005;5(4):263-274.
49. Sakaguchi S. Naturally arising Foxp3-expressing CD25+CD4+ regulatory T cells in immunological tolerance to self and non-self. *Nat Immunol.* 2005; 6(4):345-352.
50. Gooden MJ, de Bock GH, Leffers N, Daemen T, Nijman HW. The prognostic influence of tumour-infiltrating lymphocytes in cancer: a systematic review with meta-analysis. *Br J Cancer.* 2011; 105(1):93-103.
51. Maury S, Lemoine FM, Hicheri Y, et al. CD4+ CD25+ regulatory T cell depletion improves the graft-versus-tumor effect of donor lymphocytes after allogeneic hematopoietic stem cell transplantation. *Sci Transl Med.* 2010;2(41): 41ra52.
52. Mold JE, Venkatasubrahmanyam S, Burt TD, et al. Fetal and adult hematopoietic stem cells give rise to distinct T cell lineages in humans. *Science.* 2010;330(6011):1695-1699.
53. Copley MR, Babovic S, Benz C, et al. The Lin28b-let-7-Hmga2 axis determines the higher self-renewal potential of fetal haematopoietic stem cells. *Nat Cell Biol.* 2013;15(8):916-925.
54. Gardiner CM, Meara AO, Reen DJ. Differential cytotoxicity of cord blood and bone marrow-derived natural killer cells. *Blood.* 1998;91(1): 207-213.
55. Xing D, Ramsay AG, Gribben JG, et al. Cord blood natural killer cells exhibit impaired lytic immunological synapse formation that is reversed with IL-2 exvivo expansion. *J Immunother.* 2010; 33(7):684-696.